

# Effect of additional magnesium on mechanical and high-cycle fatigue properties of 6061-T6 alloy



Yoshimasa Takahashi<sup>a,\*</sup>, Takahiro Shikama<sup>b</sup>, Ryota Nakamichi<sup>a,1</sup>, Yuji Kawata<sup>a</sup>, Naoki Kasagi<sup>a,2</sup>, Hironari Nishioka<sup>a</sup>, Syuzaburo Kita<sup>a</sup>, Masanori Takuma<sup>a</sup>, Hiroshi Noguchi<sup>c</sup>

<sup>a</sup> Department of Mechanical Engineering, Kansai University, 3-3-35 Yamate-cho, Suita-shi, Osaka 564-8680, Japan

<sup>b</sup> Kobe Steel Ltd., Aluminum & Copper Business (Chofu Works), 14-1 Chofu Minato-machi, Shimonoseki, Yamaguchi 752-0953, Japan

<sup>c</sup> Department of Mechanical Engineering, Kyushu University, 744 Motoooka, Nishi-ku, Fukuoka 819-0395, Japan

## ARTICLE INFO

### Article history:

Received 27 March 2015

Received in revised form

16 June 2015

Accepted 17 June 2015

Available online 20 June 2015

### Keywords:

6061-T6 alloys

Solute magnesium

Work-hardening

Strain-aging

Fatigue limit

Coaxing effect

## ABSTRACT

The effect of additional solute magnesium (Mg) on mechanical and high-cycle-fatigue properties of 6061-T6 aluminum alloy is investigated in detail. By adding 0.5% and 0.8% Mg to the 6061-T6 alloy with a normal stoichiometric  $\text{Mg}_2\text{Si}$  composition (base alloy), the alloy exhibits eminent strain-aging characteristics demonstrated by the emergence of serrated flow, the negative strain-rate-sensitivity and relatively weakened temperature dependency of flow stress. The Mg-added new alloy also shows higher work-hardening rate than the base alloy particularly at initial flow regime and at lower strain rate. The  $S-N$  curve of the new alloy shows a clear fatigue limit which is absent in the base alloy. The fatigue limit of the new alloy is shown to be controlled by the threshold against small crack growth. Moreover, the new alloy clearly exhibits a coaxing phenomenon (time-dependent strengthening) which is absent in the base alloy. The coaxing effect is attributed to the existence of a small quasi-non-propagating crack whose growth resistance gradually increases during stress amplitude step-ups.

© 2015 Elsevier B.V. All rights reserved.

## 1. Introduction

The growing need for weight reduction of structural components has remarkably increased the demand for high strength Aluminum (Al) alloys over the past decade particularly in automobile or railroad industries. The 6061 alloy, a representative Al–Mg–Si (6XXX) alloy, is one of such material class whose matrix can be age-hardened with precipitates of magnesium-silicide ( $\text{Mg}_2\text{Si}$ ) [1]. Despite its high specific strength, the high-cycle-fatigue (HCF) property of artificially aged 6061 (6061-T6) is inferior to conventional ferrous alloys in terms of fatigue limit; the stress-life ( $S-N$ ) curve of 6061-T6 shows no distinct knee-point around  $10^5$ – $10^6$  cycles [1–4] like other non-ferrous pure face-centered-cubic (FCC) alloys. The absence of a clear threshold in HCF regime hence necessitates the introduction of a finite life strength (typically at  $5 \times 10^7$ – $10^8$  cycles for Al alloys [5]) to fatigue design, which has long been accepted as an inevitable engineering compromise while the cost of data acquisition is monumental.

In order to change such a longstanding paradigm, several of the authors began to develop a new 6061-based prototype alloy and investigated its HCF property [6,7]. The concept of the new alloy was to artificially control the appearance of a distinct fatigue limit through the addition of a strain-aging capability. Such an idea originally came from a well-known classical theory regarding the fatigue limit in ferrous alloys containing interstitials such as carbon (C) or nitrogen (N) [8–11]. Since possible interstitials (e.g. boron (B), C, N) were known to show hardly any solubility in Al matrix at room temperature [12], the addition of strain-aging capability to 6061-T6 alloy had to be achieved in a different way. Then it was found that the addition of small amount of substitutional element (Mg) to the normal 6061-T6 alloy with a stoichiometric  $\text{Mg}_2\text{Si}$  composition successfully induced the Portevin–Le Chatelier (P–L) effect and, surprisingly, a distinct fatigue limit when specimen with a small artificial defect was used [6]. Such a discovery (or more mildly termed an *interesting similarity* to ferrous alloys) had never been explicitly reported to the best of authors' knowledge.

Although the novelty and importance of the above phenomenon have been rapidly indicated in the previous short note [6], the contents of the investigation remained rather introductory; it

\* Corresponding author.

E-mail address: [yoshim-t@kansai-u.ac.jp](mailto:yoshim-t@kansai-u.ac.jp) (Y. Takahashi).

<sup>1</sup> Currently at Kobe Steel Ltd.

<sup>2</sup> Currently at Suzuki Motor Corporation Ltd.

lacked e.g. the detailed information on the strain-aging property (strain rate/temperature dependency), the critical comparison of the growth property of life-controlling small crack during coxing effect test, the quantification of fatigue crack growth (FCG) resistance in terms of the fracture mechanics, etc. In addition, the compositional design of the first prototype alloy, which was not necessarily optimized for thermal processing, had to be further modified for practical use.

In this paper, the authors fully supplement the previously un-addressed data and revisit the characteristic mechanical and HCF properties of the newly developed Al alloy in detail. Note that these evaluations are thoroughly conducted again by using the modified version of the new Al alloy (second prototype), which will provide not only a demonstration to the previous studies but also a reliable basis for the forthcoming studies.

## 2. Materials and methods

The chemical composition of the tested Al alloys is listed in Table 1. The new alloys contain ca. 0.5 wt% and 0.8 wt% extra Mg compared with the base alloy with a stoichiometric  $Mg_2Si$  composition ( $Mg:Si=1.73:1$ , mass ratio). The thermal process for the alloys is schematically shown in Fig. 1. The homogenized ingots were pre-heated at 723 K (450 °C) and die-extruded to form a round bar ( $\phi 23$  mm) at a velocity of  $50 \text{ mm s}^{-1}$ . During the extrusion process, the alloys were self-heated and eventually solutionized at ca. 773 K (500 °C). The base alloy was then immediately water-quenched. The new alloys, on the other hand, had to go through another solution treatment at a higher temperature of 813 K  $\times$  3.6 ks (540 °C  $\times$  1 h) because the solubility of  $Mg_2Si$  in the new alloys was significantly reduced by the extra Mg when compared with the base alloy [13–15]. This inevitably caused extreme grain coarsening (recrystallization) particularly at surface region where severe flow strain was imposed during die extrusion (see Fig. 2) [16]. Such a side effect, which eventually caused significant material loss in the previous prototype, was prevented by adding ca. 0.15% zirconium (Zr) to the alloys; the addition of Zr or scandium (Sc) has been shown to remarkably restrict grain coarsening by pinning grain boundaries [17–19]. After quenching, all alloys were age-hardened (463 K  $\times$  4.4 ks; 190 °C  $\times$  4 h) to obtain the peak hardness. The typical microstructure of the alloys is shown in Fig. 3. The grains in all alloys are either {111} or {100} oriented along the extrusion direction; see (a) and (b). The needle-like  $\beta$ ” precipitates (G.P. zone) oriented along the  $\langle 100 \rangle$  are seen in both alloys; see (c). The precipitates aligned parallel to the electron beam direction (i.e. normal to the printed surface) are shown as dots. The precipitates in the new alloy are generally finer and denser than those in the base alloy. Other information regarding grain size, hardness (both of which was measured on the cross-sectional plane normal to the extrusion direction) and 0.2% proof strength are listed in Table 2. Note that the grain size of the new alloy is somewhat larger than the base alloy owing possibly to the higher solutionization temperature. This is, however, tolerable as it has no negative effect on the resultant hardness and strength after aging treatment.

Specimens for tensile tests and fatigue tests were prepared from the above alloys. Fig. 4 shows specimen geometry. For tensile

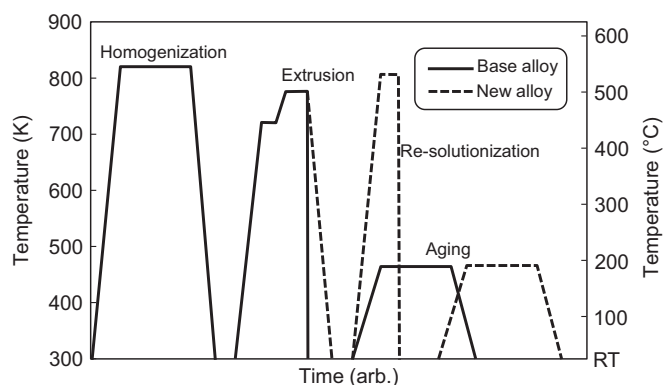


Fig. 1. Schematic diagram of heat treatment process.

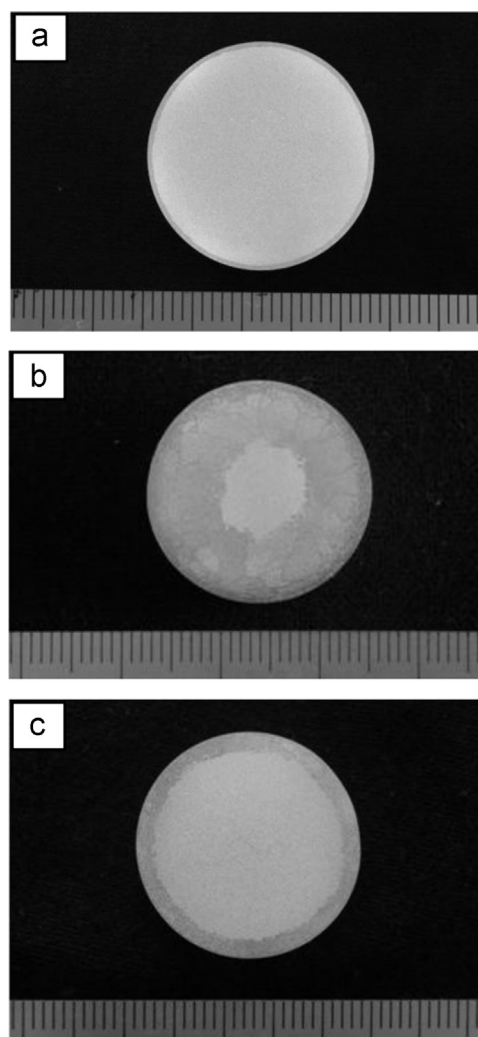


Fig. 2. Cross-sectional view of die-extruded bars: (a) base alloy (as extruded); (b) new alloy after resolutionization (0.5%Mg added, no Zr added); (c) new alloy after resolutionization (0.5%Mg and Zr added). Note that coarse grained outer region is revealed by etching (etchant: 5% sodium hydroxide solution).

Table 1  
Chemical composition of Al alloys (wt%) measured by ICP method

	Si	Fe	Cu	Mn	Mg	Cr	Ti	Zr	Al
Base alloy	0.52	0.20	0.20	0.09	0.95	0.23	0.02	–	bal.
0.5%Mg <sup>*</sup> added alloy	0.54	0.19	0.20	0.09	1.43	0.25	0.02	0.16	bal.
0.8%Mg <sup>*</sup> added alloy	0.55	0.23	0.22	0.09	1.92	0.25	0.02	0.14	bal.

\* Nominal quantity

tests, dog-bone shaped specimens having gauge length and diameter of 30 mm and 8 mm, respectively, were machined parallel to the extrusion direction. For fatigue tests, gauge length and diameter of 20 mm and 5 mm, respectively, were machined parallel to the extrusion direction. The gauge portion of the fatigue specimens was electropolished to remove damaged surface layer, and a small blind hole (diameter/depth: 300  $\mu\text{m}$ /300  $\mu\text{m}$ ) was

Download English Version:

<https://daneshyari.com/en/article/1574175>

Download Persian Version:

<https://daneshyari.com/article/1574175>

[Daneshyari.com](https://daneshyari.com)